

hep-ph/0006273
 RM3-TH/00-09
 DFTT 27/00
 GEF/TH-5-00

Evolution of truncated moments of singlet parton distributions

Stefano Forte,^{a, 1} Lorenzo Magnea,^b
 Andrea Piccione^{c, d} and Giovanni Ridolfi^d

^aINFN, Sezione di Roma Tre
 Via della Vasca Navale 84, I-00146 Rome, Italy

^bDipartimento di Fisica Teorica, Università di Torino and
 INFN, Sezione di Torino
 Via P. Giuria 1, I-10125 Torino, Italy

^cDipartimento di Fisica, Università di Genova and
^dINFN, Sezione di Genova,
 Via Dodecaneso 33, I-16146 Genova, Italy

Abstract

We define truncated Mellin moments of parton distributions by restricting the integration range over the Bjorken variable to the experimentally accessible subset $x_0 \leq x \leq 1$ of the allowed kinematic range $0 \leq x \leq 1$. We derive the evolution equations satisfied by truncated moments in the general (singlet) case in terms of an infinite triangular matrix of anomalous dimensions which couple each truncated moment to all higher moments with orders differing by integers. We show that the evolution of any moment can be determined to arbitrarily good accuracy by truncating the system of coupled moments to a sufficiently large but finite size, and show how the equations can be solved in a way suitable for numerical applications. We discuss in detail the accuracy of the method in view of applications to precision phenomenology.

June 2000

¹On leave from INFN, Sezione di Torino, Italy

1 The use of truncated moments

The needs of accurate phenomenology at current and future hadron colliders have recently led to the development of more refined tools for the QCD analysis of collider processes [1]. A detailed understanding of parton distributions and their scaling violations is in particular an essential ingredient of such phenomenology [1, 2]. Scaling violations of parton distributions are described by renormalization group equations for matrix elements of leading twist operators, whose anomalous dimensions are currently fully known to next-to-leading order [3], and to next-to-next-to-leading order for a handful of operators [4]. Moments of parton distributions are related to moments of deep-inelastic structure functions by Wilson coefficients, which have also been computed up to next-to-next-to-leading order [5]. Moments of structure functions, however, cannot be measured even indirectly, since they are defined as integrals over all kinematically allowed values of x , and thus require knowledge of the structure function for arbitrarily small x , *i.e.* arbitrarily large energy.

There is of course a well-known solution to this problem, which consists of using the Altarelli-Parisi equation [6] to evolve parton distributions directly: the scale dependence of any parton distribution at x_0 is then determined by knowledge of parton distributions for all $x > x_0$, *i.e.*, parton evolution is causal. In fact, through a judicious choice of factorization scheme [7, 8] all parton distributions can be identified with physical observables, and it is then possible to use the Altarelli-Parisi equations to express the scaling violations of structure functions entirely in terms of physically observable quantities. It is, however, hard to measure local scaling violations of structure functions in all the relevant processes: in practice, a detailed comparison with the data requires the solution of the evolution equations

What is usually done instead is to introduce a parametrization of parton distributions, and then solve the evolution equations in terms of this parametrization. The idea is that a parametrization fitted to the data will reproduce them in the experimentally accessible region, but it will also provide an extrapolation, so that the evolution equations can be solved easily, for instance taking Mellin moments. The results in the measured region should be independent of this extrapolation since, by the Altarelli-Parisi equation, measured scaling violations are independent of it. It has however become increasingly clear that in practice this procedure introduces a potentially large theoretical bias, whose exact size is very hard to assess [2, 9]. First, the very fact of adopting a specific functional form constrains not only the extrapolation in the unmeasured region, but also the allowed behavior at the boundary of the measured region. Especially when data are not very precise, it can be seen explicitly [10] that rather different results are obtained simply by changing the functional form used to parametrize parton distributions. Furthermore, it is very hard to assess the uncertainty on the best-fit functional form of the parton distributions, essentially because of the very nonlinear and indirect relation between the data and the quantity which is parametrized. Hence, the need to go through such a parametrization makes it very hard to assess the uncertainty on the desired result.

Various methods to overcome these problems have been discussed in the literature. One possibility is to minimize the bias introduced by the parton parametrization, by projecting parton distributions on an optimized basis of functions, such as suitable families of orthogonal polynomials [11]. A more ambitious proposal is to construct the probability functional for parton distributions through Bayesian inference applied on a Monte Carlo sampling of the relevant

space of functions [9]. The probability functional then summarizes in an unbiased way all the available experimental information, and can be used to determine the mean value and error on any physical observable. For many applications, however, there is a simpler, although more limited option, which consists of dealing directly with the experimentally accessible quantities. Indeed, consider two typical problems in the study of scaling violations: the determination of α_s , and the determination of a moment of the gluon distribution, for instance the first moment of the polarized gluon distribution [10], which gives the gluon spin fraction. Manifestly, in the latter case only the contribution to the moment from the measured region $x_0 \leq x \leq 1$ is accessible experimentally, and it would be useful to be able to separate in a clean way the measured quantity from the extrapolation to the unmeasured region, which is necessarily based on assumptions. It is then natural to study the scaling violation of these measurable contributions to Mellin moments, *i.e.* truncated moments. Similarly, α_s can be determined from the evolution equation of truncated moments [12], without any reference to the behavior of the structure function in the region in which it is not measured, and in principle without the need to resort to a specific functional parametrization.

It turns out [12] that scaling violations of truncated moments are described by a triangular matrix of anomalous dimensions which couple the n -th truncated moment to all truncated moments of order $n + k$, where k runs over positive integers. This means that truncated moments share with full moments the property that evolution equations are ordinary first-order differential equations, and not integro-differential equations, as for the parton distributions themselves. Unlike full moments, however, truncated moments can be measured without extrapolations. The price to pay for this is that their evolution equations do not decouple (unlike the case of full moments); however, the causal nature of the evolution implies that the evolution of each moment is only affected by higher order moments. Furthermore, the series of couplings to higher moments converges, and thus it can be truncated to any desired accuracy. The problem then reduces to the solution of a system of ordinary differential equations coupled by a triangular matrix, whose initial conditions are (measurable) truncated moments.

This gives a simple solution to both problems mentioned above: α_s and the truncated moment of the gluon can be determined directly from the observed scaling violations, without having to go through an intermediate parton parametrization. A model independent error analysis can then be performed, provided only that data for the truncated moments and their errors are available. Of course, these could be extracted directly by summing over experimental bins, if a sufficiently abundant data set were available. In practice, however, it is more convenient to manipulate a smooth interpolation of the data. It turns out to be possible to do this without invoking an explicit functional parametrization for the measured structure functions, by constructing neural networks which are trained to simulate all available experimental information, including statistical and systematic errors and correlations. By means of these neural networks it is then easy to compute the observed truncated moments and their errors, which can be further used to perform a phenomenological analysis of scaling violations, free of theoretical bias. The application of the method of neural networks to the parametrization of structure functions is currently under way and will be presented in a separate publication.

Evolution equations for truncated moments were presented in ref. [12] in the simplest (non-singlet) case, along with a preliminary study of the viability of the method. It is the purpose of this work to present a full treatment of the method of truncated moments, suitable for future

phenomenological applications. In particular, in sect. 2 we will derive evolution equations for truncated moments in the general (singlet) case, and we will discuss their solution in a form which is suitable for numerical implementation. In sect. 3 we will consider numerical solutions of the evolution equations with typical quark and gluon distributions, and discuss the accuracy of the truncation of the infinite system of coupled evolution equations. Problems and techniques of interest for future phenomenological applications are discussed in sect. 4. The appendices collect various technical results which are needed for the actual implementation of the methods discussed here in an analysis code: in particular, we give explicit expressions for the NLO singlet splitting functions in the DIS scheme, and we list all the integrals needed to compute their truncated moments.

2 Evolution equations for truncated moments and their solutions

The Q^2 dependence of parton distributions $q(x, Q^2)$ is governed by the Altarelli-Parisi (AP) equations [6]

$$\frac{d}{dt} q(x, Q^2) = \frac{\alpha_s(Q^2)}{2\pi} \int_x^1 \frac{dy}{y} P\left(\frac{x}{y}; \alpha_s(Q^2)\right) q(y, Q^2), \quad (2.1)$$

where $t = \log Q^2/\Lambda^2$. In the non-singlet case, q is simply one of the flavour non-singlet combinations of quark distributions, and P the corresponding splitting function. In the singlet case, q is a vector, whose components are the flavour-singlet combination of quark distributions,

$$\Sigma(x, Q^2) = \sum_{i=1}^{n_f} q_i(x, Q^2) \quad (2.2)$$

and the gluon distribution $g(x, Q^2)$. Correspondingly, P is a 2×2 matrix of splitting functions, given as an expansion in powers of α_s .

As is well known, upon taking ordinary Mellin moments convolutions turn into ordinary products and evolution equations become ordinary first-order differential equations. By contrast, we are interested in the evolution of truncated moments, defined for a generic function $f(x)$ by

$$f_n(x_0) = \int_{x_0}^1 dx x^{n-1} f(x). \quad (2.3)$$

The corresponding evolution equations in the nonsinglet case were derived in ref. [12], which we will follow in presenting the generalization to the singlet case. One finds immediately that the truncated moments of $q(x, Q^2)$ obey the equation

$$\frac{d}{dt} q_n(x_0, Q^2) = \frac{\alpha_s(Q^2)}{2\pi} \int_{x_0}^1 dy y^{n-1} G_n\left(\frac{x_0}{y}\right) q(y, Q^2), \quad (2.4)$$

where

$$G_n(x) = \int_x^1 dz z^{n-1} P(z) \quad (2.5)$$

is perturbatively calculable as a power series in α_s .

Expanding $G_n(x_0/y)$ in powers of y around $y = 1$,

$$G_n\left(\frac{x_0}{y}\right) = \sum_{p=0}^{\infty} \frac{g_p^n(x_0)}{p!} (y-1)^p; \quad g_p^n(x_0) = \left[\frac{\partial^p}{\partial y^p} G_n\left(\frac{x_0}{y}\right) \right]_{y=1}, \quad (2.6)$$

one obtains

$$\frac{d}{dt} q_n(x_0, Q^2) = \frac{\alpha_s(Q^2)}{2\pi} \sum_{p=0}^{\infty} \sum_{k=0}^p \frac{(-1)^{k+p} g_p^n(x_0)}{k!(p-k)!} q_{n+k}(x_0, Q^2). \quad (2.7)$$

The key step in the derivation of eq. (2.7) is the term-by-term integration of the series expansion. This is allowed, despite the fact that the radius of convergence of the series in eq. (2.6) is $1 - x_0$, because the singularity of $G_n(x_0/y)$ at $y = x_0$ is integrable (this can be proven [13] using the Lebesgue definition of the integral). One can then express each power of $(y-1)$ using the binomial expansion, which leads to eq. (2.7).

Equation (2.7) expresses the fact that, while full moments of parton distributions evolve independently of each other, truncated moments obey a system of coupled evolution equations. In particular, the evolution of the n^{th} moment is determined by all the moments q_j , with $j \geq n$. In practice, the expansion in eq. (2.6), because of its convergence, can be truncated to a finite order $p = M$. The error associated with this procedure will be discussed in sect. 3. In this case, eq. (2.7) can be rewritten as

$$\frac{d}{dt} q_n(x_0, Q^2) = \frac{\alpha_s(Q^2)}{2\pi} \sum_{k=0}^M c_{nk}^{(M)}(x_0) q_{n+k}(x_0, Q^2), \quad (2.8)$$

where

$$c_{nk}^{(M)}(x_0) = \sum_{p=k}^M \frac{(-1)^{p+k} g_p^n(x_0)}{k!(p-k)!}. \quad (2.9)$$

To solve the system of equations (2.8), it is necessary to include a decreasing number of terms (M , $M-1$, and so on) in the evolution equations for higher moments ($n+1$, $n+2$, \dots), obtaining $M+1$ equations for the $M+1$ truncated moments $\{q_n, \dots, q_{n+M}\}$. We will see in the next section that this approximation is fully justified. In this case, the coupled system of evolution equations takes the form

$$\frac{d}{d\tau} q_k = \sum_{l=n}^{n+M} C_{kl} q_l; \quad n \leq k \leq n+M, \quad (2.10)$$

with

$$\tau = \int_{t_0}^t dt' a(t'); \quad a(t) = \frac{\alpha_s(Q^2)}{2\pi}, \quad (2.11)$$

where C is now a triangular matrix:

$$\begin{cases} C_{kl} = c_{k,l-k}^{(M-k+n)} & (l \geq k) \\ C_{kl} = 0 & (l < k) \end{cases}, \quad (2.12)$$

In the nonsinglet case, discussed in ref. [12], the matrix elements C_{kl} are just numbers, and the matrix C in eq. (2.12) is triangular, which makes it easy to solve eq. (2.10) perturbatively. In the singlet case, all the steps leading to eq. (2.12) are formally the same, but now each entry C_{kl} is a 2×2 matrix. As a consequence, the matrix C , which is given in terms of truncated moments of the evolution kernels, is no longer triangular, but has nonvanishing 2×2 blocks along the diagonal. This problem can be circumvented, by writing the perturbative expansion of C as

$$C = C_0 + aC_1 + \dots = (A_0 + B_0) + a(A_1 + B_1) + \dots, \quad (2.13)$$

where $A = A_0 + aA_1$ is block-diagonal, with 2×2 blocks on its diagonal,

$$A_{kl} = C_{kk}\delta_{kl}, \quad (2.14)$$

while $B = B_0 + aB_1$, considered as a matrix of 2×2 blocks, is upper-triangular with vanishing diagonal entries. Now one can define a matrix S that diagonalizes A_0 ,

$$SA_0S^{-1} = \text{diag}(\gamma_1, \dots, \gamma_{2M}). \quad (2.15)$$

Clearly, S is τ -independent, block-diagonal, and easily computed. Equation (2.10) can then be rewritten as

$$\frac{d}{d\tau} \tilde{q} = T \tilde{q}, \quad (2.16)$$

where $\tilde{q} = S q$ and $T = SCS^{-1}$.

The new evolution matrix T is triangular at leading order (with the same eigenvalues as A_0). This is enough to solve the evolution equation to next-to-leading order, as in the nonsinglet case of ref. [12]. The general solution is worked out in detail in Appendix A; the result is

$$\tilde{q}(\tau) = U(T, \tau) \tilde{q}(0), \quad (2.17)$$

where

$$\begin{aligned} U_{ij}(T, \tau) &= R_{ik}^{-1} \left\{ \delta_{kl} \left(\frac{a(0)}{a(\tau)} \right)^{\gamma_l/b_0} \right. \\ &+ \left. \frac{\hat{T}_1^{kl} - b_1 \gamma_l \delta_{kl}}{\gamma_k - \gamma_l + b_0} \left[a(0) \left(\frac{a(0)}{a(\tau)} \right)^{\gamma_k/b_0} - a(\tau) \left(\frac{a(0)}{a(\tau)} \right)^{\gamma_l/b_0} \right] \right\} R_{lj}. \end{aligned} \quad (2.18)$$

In eqs. (2.17,2.18), T is expanded as $T = T_0 + aT_1$; R is the matrix which diagonalizes T_0 , $RT_0R^{-1} = \text{diag}(\gamma_1, \dots, \gamma_{2M})$; finally, $\hat{T}_1 = RT_1R^{-1}$.

The matrix R can be computed recursively, using the technique applied in ref. [12] and proven in Appendix B. One finds

$$R_{ij} = \frac{1}{\gamma_i - \gamma_j} \sum_{p=i}^{j-1} R_{ip} T_0^{pj}, \quad (2.19)$$

$$R_{ij}^{-1} = \frac{1}{\gamma_j - \gamma_i} \sum_{p=i+1}^j T_0^{ip} R_{pj}^{-1}, \quad (2.20)$$

which, together with the conditions $R_{ii} = 1$ and $R_{ij} = 0$ when $i > j$, determine the matrix R completely.

The general solution for the parton distributions is then

$$q(\tau) = U(C, \tau) q(0), \quad (2.21)$$

where

$$U(C, \tau) = S^{-1} U(T, \tau) S. \quad (2.22)$$

The splitting functions and truncated moment integrals which should be used in eq. (2.18) in order compute this solution explicitly are listed in Appendices C and D.

For the sake of completeness, we describe a different method to solve eq. (2.8). It is immediate to check that the matrix

$$U(C, \tau) = I + \sum_{n=1}^{\infty} \int_0^{\tau} d\tau_1 \dots \int_0^{\tau_{n-1}} d\tau_n C(\tau_1) \dots C(\tau_n) \quad (2.23)$$

obeys the differential equation

$$\frac{d}{d\tau} U(C, \tau) = C U(C, \tau), \quad (2.24)$$

with the initial condition $U(C, 0) = I$. In general, eq. (2.23) is not very useful, since it involves an infinite sum. In the present case, however, the infinite sum collapses to a finite sum. To see this, consider again the decomposition $C = A + B$, where A is block-diagonal and B is upper-triangular. It is easy to prove that

$$U(C, \tau) = U(A, \tau) U(\tilde{B}, \tau), \quad (2.25)$$

where

$$\tilde{B} = U^{-1}(A, \tau) B U(A, \tau). \quad (2.26)$$

Since A is block diagonal, $U(A, \tau)$ is also block-diagonal, and it can be computed perturbatively using the procedure described in Appendix A. Furthermore, once $U(A)$ is known, the upper-triangular matrix \tilde{B} can be computed through eq. (2.26). Now one can use the fact that upper-triangular matrices have the property that their M -th power vanishes. Hence, the solution can be expressed as the finite sum

$$U(\tilde{B}, \tau) = I + \sum_{n=1}^{M-1} \int_0^{\tau} d\tau_1 \dots \int_0^{\tau_{n-1}} d\tau_n \tilde{B}(\tau_1) \dots \tilde{B}(\tau_n), \quad (2.27)$$

and from the knowledge of $U(\tilde{B})$ and $U(A)$ one can determine the solution to the evolution equations explicitly.

3 Numerical methods and their accuracy

In this section we will assess the accuracy of our method when the series of contributions to the right-hand side of the evolution equation (2.7) is approximated by retaining a finite number M of terms. The loss of accuracy due to this truncation is the price to pay for eliminating the dependence on parton parametrizations and extrapolations in the unmeasured region. However, unlike the latter uncertainties, which are difficult to estimate, the truncation uncertainty can be simply assessed by studying the convergence of the series. A reasonable goal, suitable for state-of-the-art phenomenology, is to reproduce the evolution equations to about 5% accuracy: indeed, we expect the uncertainties related to the parametrization of parton distributions in the conventional approach to be somewhat larger ($\sim 10\%$)¹. Notice that there is no obstacle to achieve a higher level of precision when necessary, by simply including more terms in the relevant expansions. To this level of accuracy it is enough to study the behavior of the leading order contribution to the evolution equation: indeed, next-to-leading corrections to the anomalous dimension are themselves of order 10%. We have verified explicitly that the inclusion of the next-to-leading corrections does not affect our conclusions.

We can compare the exact evolution equation (2.7) with its approximate form, eq. (2.8), by defining the percentage error on the right-hand side of the evolution equations for the quark nonsinglet, singlet and gluon:

$$\mathcal{R}_{n,M}^{NS} = \frac{1}{\mathcal{N}_{NS}} \int_{x_0}^1 dy y^{n-1} \left[G_n^{NS} \left(\frac{x_0}{y} \right) - \sum_{k=0}^M y^k c_{nk}^{NS} \right] q^{NS}(y, Q^2), \quad (3.1)$$

$$\begin{aligned} \mathcal{R}_{n,M}^{\Sigma} = \frac{1}{\mathcal{N}_{\Sigma}} \int_{x_0}^1 dy y^{n-1} & \left\{ \left[G_n^{qq} \left(\frac{x_0}{y} \right) - \sum_{k=0}^M y^k c_{nk}^{qq} \right] \Sigma(y, Q^2) \right. \\ & \left. + \left[G_n^{qg} \left(\frac{x_0}{y} \right) - \sum_{k=0}^M y^k c_{nk}^{qg} \right] g(y, Q^2) \right\}, \end{aligned} \quad (3.2)$$

$$\begin{aligned} \mathcal{R}_{n,M}^g = \frac{1}{\mathcal{N}_g} \int_{x_0}^1 dy y^{n-1} & \left\{ \left[G_n^{gg} \left(\frac{x_0}{y} \right) - \sum_{k=0}^M y^k c_{nk}^{gg} \right] \Sigma(y, Q^2) \right. \\ & \left. + \left[G_n^{gg} \left(\frac{x_0}{y} \right) - \sum_{k=0}^M y^k c_{nk}^{gg} \right] g(y, Q^2) \right\}, \end{aligned} \quad (3.3)$$

where $\mathcal{N}_{NS, \Sigma, g}$ are the exact right-hand sides of the evolution equation (2.7). We study the dependence of the percentage error on the value of M for typical values of the cutoff x_0 and for representative choices of test parton distributions. In particular, we parametrize parton distributions as

$$q(x, Q^2) = Nx^{-\alpha}(1-x)^{\beta}. \quad (3.4)$$

We begin by choosing, as a representative case, $\beta = 4$ and $\alpha = 1$ for the singlet distributions and $\alpha = 0$ for the nonsinglet. The nonsinglet is assumed to behave qualitatively as $q_{NS} \sim xg \sim x\Sigma$, in accordance with the behavior of the respective splitting functions. Furthermore,

¹Notice that this is *not* the uncertainty associated with evolution of a *given* parametrization with, say, an x -space code; rather, it is the uncertainty associated with the *choice* of the parametrization, and with the bias it introduces in the shape of the distribution.

the normalization factors N for the singlet and gluon are fixed by requiring that the second moments of $\Sigma(x, Q^2)$ and $g(x, Q^2)$ are in the ratio 0.6/0.4, which is the approximate relative size of the quark and gluon momentum fractions at a scale of a few GeV². We will then show that changing the values of α and β within a physically reasonable range does not affect the qualitative features of our results.

The accuracy of the truncation of the evolution equation is determined by the convergence of the expansion in eq. (2.6). Because this expansion is centered at $y = 1$, and diverges at $y = x_0$, the small y region of the integration range in eq. (2.4) is poorly reproduced by the expansion. Hence, even though the series in eq. (2.7) converges, as discussed in sect. 2, the convergence will be slower for low moments, which receive a larger contribution from the region of integration $y \sim x_0$. In fact, for low enough values of n , the convolution integral on the right-hand side of the evolution equation (2.4) does not exist: this happens for the same value for which the full moment of the structure function does not exist, *i.e.* $n \leq 1$ in the unpolarized singlet and $n \leq 0$ in the unpolarized nonsinglet and in the polarized case. Therefore, we concentrate on the lowest existing integer moments of unpolarized distributions, *i.e.* the cases $n = 2, 3$ for the singlet distributions, and correspondingly $n = 1, 2$ for the nonsinglet, which are the cases in which the accuracy of the truncation will be worse.

The values of $\mathcal{R}_{n,M}^{NS,\Sigma,g}$, computed at leading order with $x_0 = 0.1$, are shown in table 1. The

$x_0 = 0.1$						
M	$\mathcal{R}_{1,M}^{NS}$	$\mathcal{R}_{2,M}^{\Sigma}$	$\mathcal{R}_{2,M}^g$	$\mathcal{R}_{2,M}^{NS}$	$\mathcal{R}_{3,M}^{\Sigma}$	$\mathcal{R}_{3,M}^g$
5	0.63	0.43	0.55	0.16	0.12	0.16
10	0.49	0.36	0.38	0.13	0.10	0.12
20	0.34	0.27	0.26	0.10	0.08	0.08
40	0.20	0.17	0.17	0.06	0.05	0.05
70	0.12	0.10	0.10	0.04	0.03	0.03
100	0.09	0.07	0.07	0.03	0.02	0.02
150	0.06	0.05	0.05	0.02	0.01	0.01

Table 1: *Values of $\mathcal{R}_{n,M}^{NS,\Sigma,g}$ for $x_0 = 0.1$ and different values of n and M .*

table shows that nonsinglet moments of order n behave as singlet moments of order $n - 1$. This is a consequence of the fact that, as discussed above, the convergence of the expansion is determined by the singularity of the integrand $G_n(x_0/y) q(y)$ of eq. (2.4) as $y \rightarrow x_0$; near $y = x_0$, the function $G_n(x_0/y)$ is well approximated by the singular contribution $\log(1 - x_0/y)$, while parton distributions carry an extra power of y^{-1} in the singlet case in comparison to the nonsinglet. We also observe in table 1 that, as expected, the convergence is slower for the lowest moments, and rapidly improves as the order of the moment increases. This rapid improvement is a consequence of the fact that the convergence of the expansion of $G(x_0/y)$ is only slow in the immediate vicinity of the point $y = x_0$, and the contribution of this region to the n -th moment is suppressed by a factor of x_0^{n-1} . Due to this fast improvement, the approximation introduced by including one less term in the expansion as the order of the moment is increased by one, which is necessary to obtain the closed system of evolution equations (2.10), is certainly

justified.

The 5% accuracy goal which we set to ourselves requires the inclusion of more than 100 terms for the lowest moment, but only about 40 terms for the next-to-lowest. The computation of series with such a large number of contributions does not present any problem, since the splitting functions are known and their truncated moments are easily determined numerically. The implications of this requirement for phenomenology will be discussed in the next section.

We can now study the dependence of these results on the value of the truncation point x_0 by plotting the exact and approximate right-hand side of the evolution equations as a function of x_0 , as shown in fig. 1. The figures show that the case $x_0 = 0.1$ studied in table 1 is a generic one between the two limiting (and physically uninteresting) cases $x_0 = 0$ and $x_0 = 1$, where the approximation is exact. In fact, with this particular choice of parton distributions, $x_0 = 0.1$ is essentially a worst case and the error estimates of table 1 are therefore conservative.

An interesting feature of these plots is the presence of zeroes of the lowest moment evolution at $x_0 = 0$ in the nonsinglet and around $x_0 \approx 10^{-2}$ in the gluon case. The physical origin of these zeroes is clear. At leading order, the first nonsinglet full moment does not evolve. On the other hand, the second gluon full moment grows with Q^2 , while higher gluon full moments decrease, *i.e.* the gluon distribution decreases at large x ; this implies that the second truncated moment of the gluon must decrease for a high enough value of the cutoff x_0 , while it must increase for very small x_0 ; its derivative is thus bound to vanish at some intermediate point. Of course, the phenomenology of scaling violations (such as a determination of α_s) cannot be performed at or close to these zeroes, where there is no evolution. From the point of view of a truncated moment analysis, this means that the value of x_0 should be chosen with care in order to avoid these regions.

Finally, in table 2 we study the dependence of our results on the form of the parton distributions, by varying the parameters α and β within a reasonable range. Of course, parton distributions which are more concentrated at small y give rise to slower convergence. However, we can safely conclude that the effect of varying the shape of parton distributions is generally rather small. We have also verified that varying the relative normalization of the quark and gluon distributions has a negligible effect on the convergence of the series, even though it may change by a moderate amount the position of the zeroes in gluon evolution discussed above.

4 Techniques for phenomenological applications

So far we have discussed scaling violations of parton distributions. In a generic factorization scheme, the measured structure functions are convolutions of parton distributions and coefficient functions. When taking moments, convolutions turn into ordinary products and moments of coefficient functions are identified with Wilson coefficients. In the present case, however, as shown in eqs. (2.4-2.7), truncated moments turn convolutions into products of triangular matrices. Hence, in a generic factorization scheme, truncated moments of parton distributions are related to truncated moments of structure functions by a further triangular matrix of truncated moments of coefficient functions.

This complication can be avoided by working in a parton scheme [7], where the quark distribution is identified with the structure function F_2 . This still does not fix the factorization

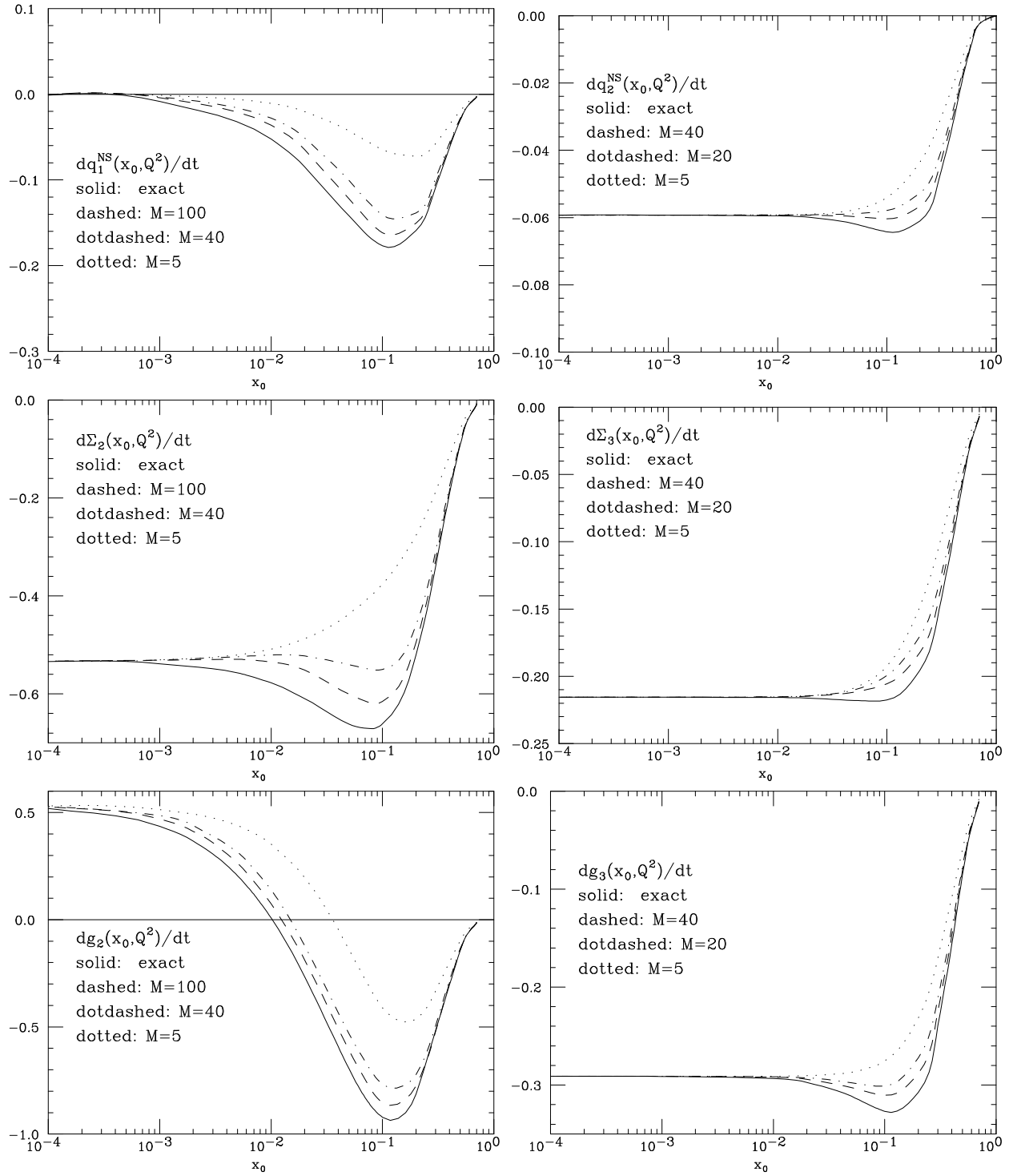


Figure 1: Right-hand sides of the evolution equations for the first and second truncated moments of the nonsinglet distribution, and for the second and third moments of singlet distributions. The overall scale is set by $\alpha_s(2 \text{ GeV}^2)$.

$n = 2, x_0 = 0.1$					
α	β	$\mathcal{R}_{n,20}^\Sigma$	$\mathcal{R}_{n,70}^\Sigma$	$\mathcal{R}_{n,20}^g$	$\mathcal{R}_{n,70}^g$
1.5	2.0	0.26	0.10	0.27	0.11
1.0	2.0	0.20	0.07	0.23	0.09
0.5	2.0	0.14	0.05	0.18	0.07
1.5	4.0	0.32	0.12	0.30	0.12
1.0	4.0	0.27	0.10	0.26	0.10
0.5	4.0	0.22	0.08	0.22	0.09
1.5	6.0	0.36	0.14	0.32	0.14
1.0	6.0	0.32	0.12	0.29	0.12
0.5	6.0	0.27	0.10	0.26	0.10
$n = 3, x_0 = 0.1$					
α	β	$\mathcal{R}_{n,20}^\Sigma$	$\mathcal{R}_{n,70}^\Sigma$	$\mathcal{R}_{n,20}^g$	$\mathcal{R}_{n,70}^g$
1.5	2.0	0.07	0.03	0.07	0.03
1.0	2.0	0.04	0.02	0.04	0.02
0.5	2.0	0.02	0.01	0.02	0.01
1.5	4.0	0.12	0.05	0.11	0.05
1.0	4.0	0.08	0.03	0.08	0.03
0.5	4.0	0.05	0.02	0.05	0.02
1.5	6.0	0.16	0.07	0.15	0.06
1.0	6.0	0.12	0.05	0.12	0.05
0.5	6.0	0.09	0.03	0.08	0.03

Table 2: *Values of $\mathcal{R}_{n,M}^\Sigma$ and $\mathcal{R}_{n,M}^g$ for $x_0 = 0.1$ and different choices of parton distribution parameters.*

scheme completely in the gluon sector. One way of fixing it is to use a “physical” scheme, where all parton distributions are identified with physical observables [8]. This may eventually prove the most convenient choice for the sake of precision phenomenology, once accurate data on all the relevant physical observables are available. At present, however, the gluon distribution is mostly determined from scaling violations of F_2 , so within the parton family of schemes the choice of gluon factorization is immaterial. Here we will fix the scheme by assuming that all moments satisfy the relations between the parton–scheme gluon and the $\overline{\text{MS}}$ quark and gluons imposed by momentum conservation on second moments [14]. This is the prescription used in common parton sets, and usually referred to as DIS scheme. Explicit expressions of Altarelli-Parisi kernels in the DIS scheme are given in Appendix C.

With this prescription, the phenomenology of scaling violations can be studied by computing a sufficiently large number of truncated moments of structure functions, so as to guarantee the required accuracy. If the aim is, for instance, a determination of α_s from nonsinglet scaling violations, all we need is a large enough number of truncated moments of the nonsinglet structure function. Once an interpolation of the data in the measured region is available, the determination of such truncated moments is straightforward. This interpolation can be performed in an unbiased way using neural networks, as already mentioned in the introduction. One may

wonder, however, whether the need to use the values of very high moments wouldn't be a problem. Indeed, very high moments depend strongly on the behavior of the structure function at large y , which is experimentally known very poorly. Furthermore, it seems contradictory that scaling violations of the lowest moments should be most dependent on the structure function at large y .

This dependence is only apparent, however. Indeed, eq. (2.7) for, say, the nonsinglet first moment can be rewritten as

$$\frac{d}{dt}q_1(x_0, Q^2) = \frac{\alpha_s(Q^2)}{2\pi} \sum_{p=0}^{\infty} \frac{g_p^1(x_0)}{p!} \hat{q}_1^p(x_0, Q^2) , \quad (4.1)$$

where

$$\hat{q}_k^p(x_0, Q^2) = \int_{x_0}^1 dy y^{k-1} (y-1)^p q(y, Q^2) . \quad (4.2)$$

The need to include high orders in the expansion in eq. (2.8) is due to the slow convergence of the series in eq. (4.1), in turn determined by the fact that $G_n(x_0/y)$ diverges logarithmically at $y = x_0$. Correspondingly, the right-hand side of the evolution equation depends significantly on \hat{q}_1^p for large values of p , which signal a sensitivity to the value of $q(y, Q^2)$ in the neighborhood of the point $y = x_0$. The dependence on high truncated moments q_n is introduced when \hat{q}_1^p is re-expressed in terms of q_n , by expanding the binomial series for $(y-1)^p$. Since this re-expansion is exact, it cannot introduce a dependence on the large y region which is not there in the original expression. The high orders of the expansion do instead introduce a significant dependence on the value of the structure function in the neighborhood of x_0 , which can be kept under control provided x_0 is not too small, *i.e.* well into the measured region. There is therefore no obstacle even in practice in performing an accurate determination of α_s from scaling violations of truncated moments.

Let us now consider a second typical application of our method, namely the determination of truncated moments of the gluon distribution. In particular, the physically interesting case is the lowest integer moment, *i.e.* the momentum fraction in the unpolarized case or the spin fraction in the polarized case. The need to include a large number of terms in the expansion of the evolution equations seems to imply the need to introduce an equally large number of parameters, one for each gluon truncated moment. This would be problematic since it appears unrealistic to fit a very large number of parameters of the gluon from currently available data on scaling violations. We may, however, take advantage of the fact that the dependence on high order truncated moments is fictitious, as we have just seen, and it rather indicates an enhanced sensitivity to the value of $q(y)$ as $y \rightarrow x_0$. This suggests that a natural set of parameters to describe the gluon distribution should include the first several truncated moments, as well as further information on the behavior of the distribution around the truncation point x_0 , such as the value of the distribution (and possibly of some of its derivatives) at the point x_0 .

To understand how such a parametrization might work, notice that if $q(y)$ is regular around $y = x_0$, then it is easy to prove that

$$\lim_{p \rightarrow \infty} \frac{\int_{x_0}^1 dy (y-1)^p q(y)}{q(x_0) \int_{x_0}^1 dy (y-1)^p} = 1 , \quad (4.3)$$

by Taylor expanding $q(y)$ about $y = x_0$. We may therefore approximate the series which appears on the *r.h.s.* of eq. (4.1) by

$$S(x_0, n_0) = \sum_{p=0}^{n_0-1} \frac{g_p^1(x_0)}{p!} \int_{x_0}^1 dy (y-1)^p q(y) + \sum_{p=n_0}^{\infty} \frac{g_p^1(x_0)}{p!} q(x_0) \int_{x_0}^1 dy (y-1)^p. \quad (4.4)$$

Equation (4.4) describes the evolution of the first truncated moment of $q(y)$ in terms of the first n_0 truncated moments and of the value of $q(y)$ at the truncation point x_0 . Of course, the approximation gets better if n_0 increases. It is easy to check that when $x_0 = 0.1$ the accuracy is already better than 10% when $n_0 \sim 7$. This means that a parametrization of the distribution in terms of less than ten parameters is fully adequate. It is easy to convince oneself that this estimate is reliable, and essentially independent of the shape of the distribution $q(y)$. In fact, because slow convergence arises due to the logarithmic singularity in $G_n(x_0/y)$, we can estimate the error of the approximation in eq. (4.4) by replacing the functions $g_p^1(x_0)/p!$ with the coefficients of the Taylor expansion of $\log(1-x_0/y)$ in powers of $y-1$, which we may denote by $\hat{g}_p^1(x_0)/p!$. The error is then

$$\begin{aligned} & \left| \sum_{p=n_0}^{\infty} \frac{\hat{g}_p^1(x_0)}{p!} \int_{x_0}^1 dy (y-1)^p (q(y) - q(x_0)) \right| \\ & \leq \int_{x_0}^1 dy \left| \log(1-x_0/y) - \sum_{p=0}^{n_0-1} \frac{\hat{g}_p^1(x_0)}{p!} (y-1)^p \right| |q(y) - q(x_0)|. \end{aligned} \quad (4.5)$$

The expression inside the first absolute value on the *r.h.s.* of eq. (4.5) is just the error made in approximating the logarithm with its Taylor expansion around $y = 1$; thus, it is a slowly decreasing function of n_0 , it is integrable, and the integral receives the largest contribution from the region $y \sim x_0$; the second absolute value, on the other hand, is a bounded function of y in the range $x_0 \leq y \leq 1$, which vanishes as $y \rightarrow x_0$ for any choice of $q(y)$. These two facts combine to limit the size of the error. One can check directly that, choosing for example $q(y) = (1-y)^4$ as in the previous section, the accuracy is better than 10% with $n_0 \sim 10$ and $x_0 = 0.1$, in agreement with the previous estimate. One may also verify that, as expected, changing the shape of $q(y)$ does not significantly affect the result.

We conclude that there is no difficulty in using the evolution of truncated moments for a direct extraction of the lowest truncated moment of the gluon distribution, provided only the higher moments of the distributions, which are auxiliary quantities needed in the extraction, are parametrized in an effective way. We have seen that this is possible with a reasonably small number of parameters.

5 Outlook

In this paper, we have discussed the solution of the Altarelli-Parisi evolution equations of perturbative QCD by projecting parton distributions on a basis of truncated moments. We have seen that truncated moments give us a compromise between standard Mellin moments, which satisfy simple linear evolution equations, but are not measurable, and parton distributions

themselves, which are measurable, but satisfy integro-differential evolution equations. In this respect, projecting on a basis of truncated moments is akin to projecting on a basis of orthogonal polynomials [11], but with the added advantage that truncated moments are physical observables. We have further shown that evolution equations for truncated moments can be solved to arbitrarily high accuracy by using a sufficiently large basis of truncated moments, and we have discussed how this formalism can be exploited to perform a model-independent, unbiased analysis of scaling violations, which does not rely on parton parametrizations. We have also collected all technical tools which are needed for this analysis, and discussed the reliability of the approximations which are necessary in order to implement it in practice. Such an analysis could be used for the determination of α_s and for the direct measurement of the contribution to the moments of the gluon distribution from the experimentally accessible region. In both cases, it would offer the advantage of allowing reliable estimates of the uncertainty on the result. In order to be effective, these phenomenological applications will need an unbiased interpolation of the data, such as could be achieved by means of neural networks. Phenomenological studies along these lines are currently under investigation and will be presented in forthcoming publications.

Acknowledgements We thank Ll. Garrido and J.I. Latorre for discussions on neural networks and their applications to structure functions. We thank R. Ball for a careful reading of the manuscript and several useful comments.

A Solution of matrix evolution equations at NLO

In this Appendix, we find the general solution of the equation

$$\frac{d}{d\tau} q = C q, \quad (\text{A.1})$$

where q is a vector with M components, and C is a generic $M \times M$ matrix. The usual QCD evolution equations are special cases of this equation in which $M \leq 2$. We will assume that C has a perturbative expansion in powers of a parameter $a(\tau)$:

$$C = C_0 + a(\tau)C_1 + \dots, \quad (\text{A.2})$$

with

$$\frac{da(\tau)}{d\tau} = -b_0 a (1 + b_1 a + \dots). \quad (\text{A.3})$$

For QCD applications

$$a = \frac{\alpha_s}{2\pi}; \quad \tau = \frac{1}{2\pi} \int_{t_0}^t dt' \alpha_s(t'), \quad (\text{A.4})$$

with $t = \log(Q^2/\Lambda_{QCD}^2)$, and

$$\frac{b_0}{2\pi} = \frac{33 - 2n_f}{12\pi}; \quad \frac{b_1}{2\pi} = \frac{153 - 19n_f}{2\pi(33 - 2n_f)}. \quad (\text{A.5})$$

The solution of eq. (A.1) can be obtained perturbatively. Expanding q to order a ,

$$q = q_0 + a q_1 , \quad (\text{A.6})$$

we find

$$\frac{d}{d\tau} q_0 = C_0 q_0 , \quad (\text{A.7})$$

$$\frac{d}{d\tau} q_1 = (C_0 + b_0) q_1 + C_1 q_0 . \quad (\text{A.8})$$

The solutions of eqs. (A.7,A.8) are

$$q_0(\tau) = R^{-1} e^{\gamma\tau} R q_0(0) , \quad (\text{A.9})$$

$$q_1(\tau) = R^{-1} e^{(\gamma+b_0)\tau} R q_1(0) + R^{-1} e^{(\gamma+b_0)\tau} \int_0^\tau d\sigma e^{-(\gamma+b_0)\sigma} \hat{C}_1 e^{\gamma\sigma} R q_0(0) , \quad (\text{A.10})$$

where the matrix R diagonalizes C_0 ,

$$RC_0R^{-1} = \text{diag}(\gamma_1, \dots, \gamma_M) \equiv \gamma , \quad (\text{A.11})$$

and

$$\hat{C}_1 = RC_1R^{-1} . \quad (\text{A.12})$$

Collecting these results, and noting that $a \exp(b_0\tau) = a(0)$, up to terms of order a^2 , we can write the solution as

$$q(\tau) \equiv U(C, \tau)q(0) = R^{-1} \left[e^{\gamma\tau} + a e^{(\gamma+b_0)\tau} \int_0^\tau d\sigma e^{-(\gamma+b_0)\sigma} \hat{C}_1 e^{\gamma\sigma} \right] R q(0) , \quad (\text{A.13})$$

with the initial condition

$$q(0) = q_0(0) + a(0)q_1(0) . \quad (\text{A.14})$$

The explicit expression of $U(C, \tau)$ is

$$U_{ij}(C, \tau) = R_{im}^{-1} \left[\delta_{mn} e^{\gamma^n \tau} + a(\tau) \hat{C}_1^{mn} \frac{e^{\gamma^n \tau} - e^{(\gamma^m + b_0)\tau}}{\gamma^n - \gamma^m - b_0} \right] R_{nj} , \quad (\text{A.15})$$

which, expanded to next-to-leading order reduces to

$$\begin{aligned} U_{ij}(C, \tau) = & R_{im}^{-1} \left\{ \delta_{mn} \left(\frac{a(0)}{a(\tau)} \right)^{\gamma_n/b_0} \right. \\ & \left. + \frac{\hat{C}_1^{mn} - b_1 \gamma_n \delta_{mn}}{\gamma^m - \gamma^n + b_0} \left[a(0) \left(\frac{a(0)}{a(\tau)} \right)^{\gamma_m/b_0} - a(\tau) \left(\frac{a(0)}{a(\tau)} \right)^{\gamma_n/b_0} \right] \right\} R_{nj} . \end{aligned} \quad (\text{A.16})$$

In the case of standard QCD evolution equations the matrix C_0 is at most 2×2 and is easily diagonalized. In the cases treated in this paper, the matrix C_0 is triangular and can be diagonalized using the methods discussed in the next Appendix.

B Diagonalization of triangular matrices

In this Appendix, we show how to construct the matrix R which diagonalizes a generic $n \times n$ triangular matrix T by means of the recursion relations eqs. (2.19,2.20). The matrix R is defined by the requirement that

$$RTR^{-1} = \text{diag}(\gamma_1, \dots, \gamma_n) , \quad (\text{B.1})$$

where the matrix T is upper triangular, *i.e.* $T_{ij} = 0$ if $i > j$. It is easy to see, by solving the secular equation, that the eigenvalues γ_i of T coincide with its diagonal elements,

$$\gamma_i = T_{ii} . \quad (\text{B.2})$$

Now, define eigenvectors v^j associated to the j -th eigenvalue T_{jj} , with components v_i^j :

$$\sum_{k=1}^n T_{ik} v_k^j = \gamma_j v_i^j . \quad (\text{B.3})$$

Clearly, the matrix R^{-1} coincides with the matrix of right eigenvectors, $(R^{-1})_{ij} = v_i^j$, while the matrix R coincides with the matrix of left eigenvectors $\sum_{k=1}^n \hat{v}^j_k T_{ki} = \gamma_j \hat{v}^j_i$, $R_{ij} = \hat{v}^i_j$. The eigenvector condition eq. (B.3) immediately implies that the j -th component of the j -th eigenvector is equal to one: $v_j^j = 1$. Furthermore, it is clear that eq. (B.3) can only be satisfied if all components v_k^j of the j -th eigenvector with $k > j$ vanish,

$$v_j^j = 1 ; \quad v_k^j = 0 \quad \text{if} \quad k > j . \quad (\text{B.4})$$

Using eq. (B.4) and the fact that the matrix T is triangular, eq. (B.3) can be written as

$$\sum_{k=i}^j T_{ik} v_k^j = \gamma_j v_i^j . \quad (\text{B.5})$$

Substituting the explicit form of the eigenvalues, eq. (B.2), and identifying $v_i^j = (R^{-1})_{ij}$, this is immediately seen to coincide with eq. (2.20). Furthermore, using the condition $v_j^j = 1$, this equation can be viewed as a recursion relation which allows the determination of the $(k-1)$ -th element of v^j once the k -th element is known, which is what we set out to prove. The same argument, applied to the left eigenvectors, leads to the expression in eq. (2.19) for R .

C Splitting Functions in the DIS scheme

In this Appendix, we give the explicit expressions of the Altarelli-Parisi kernels in the DIS scheme [7, 14]. We define the non-singlet splitting functions as

$$P_{\pm}(x) \equiv P_{qq}(x) \pm P_{q\bar{q}}(x) = P_{\pm}^{(0)}(x) + aP_{\pm}^{(1)}(x) + \dots \quad (\text{C.1})$$

and the singlet 2×2 matrix of splitting functions as

$$P(x) = P^{(0)}(x) + aP^{(1)}(x) + \dots \quad (\text{C.2})$$

The $\overline{\text{MS}}$ LO and NLO kernels are given for example in eqs. (4.94) and (4.102)-(4.112) of ref. [3], whose notation and conventions we have followed throughout this paper. The splitting functions in the DIS scheme can be constructed from these by a change of factorization scheme.

To next-to-leading order, a generic change of factorization scheme for the splitting functions is

$$P_{\pm}^{(1)} \rightarrow P_{\pm}^{(1)} - b_0 E^{NS}, \quad (\text{C.3})$$

$$P^{(1)} \rightarrow P^{(1)} + [E, P^{(0)}] - b_0 E, \quad (\text{C.4})$$

where E and E^{NS} are functions of x , and the commutator in eq. (C.4) is defined in terms of convolutions, as

$$[E, P^{(0)}] = E \otimes P^{(0)} - P^{(0)} \otimes E, \quad (\text{C.5})$$

and is thus in general nontrivial to compute.

The transformation that takes from the $\overline{\text{MS}}$ to the DIS scheme, defined as in ref. [14], is given by

$$E^{NS}(x) = C^{qq}(x), \quad (\text{C.6})$$

$$E(x) = \begin{bmatrix} C^{qq}(x) & C^{qg}(x) \\ -C^{qq}(x) & -2n_f C^{qg}(x) \end{bmatrix}, \quad (\text{C.7})$$

where $C^{qq}(x)$ and $C^{qg}(x)$ are the next-to-leading terms of the quark and gluon coefficient functions for the unpolarized deep-inelastic structure function $F_2(x, Q^2)$,

$$\begin{aligned} C^{qq}(x) &= C_F \left[2 \left(\frac{\log(1-x)}{1-x} \right)_+ - \frac{3}{2} \left(\frac{1}{1-x} \right)_+ - (1+x) \log(1-x) \right. \\ &\quad \left. - \frac{1+x^2}{1-x} \log x + 3 + 2x - \left(\frac{\pi^2}{3} + \frac{9}{2} \right) \delta(1-x) \right], \end{aligned} \quad (\text{C.8})$$

$$C^{qg}(x) = T_R \left[\left((1-x^2) + x^2 \right) \log \frac{1-x}{x} - 8x^2 + 8x - 1 \right]. \quad (\text{C.9})$$

The explicit expression of the commutators is

$$\begin{aligned} [E, P^{(0)}]_{qq} &= C_F \left[- (1+x) \text{Li}_2(x) - \frac{1+x}{2} \log^2 x \right. \\ &\quad + \left(\frac{1}{2} + \frac{2}{3x} - \frac{x}{2} - \frac{2x^2}{3} \right) \log(1-x) \\ &\quad - \left(\frac{1}{2} + \frac{5x}{2} - \frac{2x^2}{3} \right) \log x - \frac{10}{3} + \frac{\pi^2}{6} + \frac{1}{3x} + \frac{x}{3} + \frac{\pi^2 x}{6} + \frac{8x^2}{3} \left. \right] \\ &\quad + C_F n_f \left[- (1-2x) \text{Li}_2(x) - \left(\frac{7}{2} - 8x + 6x^2 \right) \log(1-x) \right. \\ &\quad - (2-4x+4x^2) \log x \log(1-x) + (1-2x+2x^2) \log^2(1-x) \\ &\quad + \left(\frac{1}{2} - x + 2x^2 \right) \log^2 x - \left(\frac{1}{2} + 4x - 6x^2 \right) \log x \\ &\quad \left. - \frac{5}{2} - \frac{\pi^2}{6} + 6x + \frac{\pi^2 x}{3} - 8x^2 - \frac{2\pi^2 x^2}{3} \right], \end{aligned} \quad (\text{C.10})$$

$$\begin{aligned}
[E, P^{(0)}]_{qg} = & b_0 C^{qq}(x) + n_f^2 \left[\left(\frac{1}{2} + 2x + 2x^2 \right) \log^2 x + (1 + 4x + 4x^2) \text{Li}_2(x) \right. \\
& - (2 + 4x - 6x^2) \log(1-x) + (2 + 16x + 10x^2) \log x \\
& + \frac{11}{2} - \frac{\pi^2}{6} + 24x - \frac{2\pi^2 x}{3} - \frac{59x^2}{2} - \frac{2\pi^2 x^2}{3} \left. \right] \\
& + C_F n_f \left[- (1 - 2x) \text{Li}_2(x) - \left(\frac{7}{2} - 8x + 6x^2 \right) \log(1-x) \right. \\
& - (2 - 4x + 4x^2) \log x \log(1-x) + (1 - 2x + 2x^2) \log^2(1-x) \\
& + \left(\frac{1}{2} - x + 2x^2 \right) \log^2 x - \left(\frac{1}{2} + 4x - 6x^2 \right) \log x \\
& - \frac{5}{2} - \frac{\pi^2}{6} + 6x + \frac{\pi^2 x}{3} - 8x^2 - \frac{2\pi^2 x^2}{3} \left. \right] \\
& + C_A \left[- (1 + 4x) \text{Li}_2(x) - \left(\frac{1}{2} + 2x \right) \log^2 x \right. \\
& + \left(-\frac{1}{2} + \frac{2}{3x} + 12x - \frac{79x^2}{6} \right) \log(1-x) \\
& + (1 - 2x + 2x^2) \log(1-x) \log \frac{1-x}{x} - \left(\frac{1}{2} + 16x - \frac{31x^2}{6} \right) \log x \\
& - \frac{43}{12} + \frac{1}{3x} - \frac{121x}{6} + \pi^2 x + \frac{281x^2}{12} - \frac{\pi^2 x^2}{3} \left. \right] \\
& + C_F \left[- \left(\frac{1}{4} - 4x + 8x^2 \right) \log x - \left(\frac{1}{2} - x + 2x^2 \right) \text{Li}_2(x) \right. \\
& - (1 - 2x + 2x^2) \log(1-x) \log \frac{1-x}{x} - \left(\frac{1}{4} - \frac{x}{2} + x^2 \right) \log^2 x \\
& + \left. \left(\frac{5}{4} - 9x + 8x^2 \right) \log(1-x) - \frac{7}{4} + \frac{\pi^2}{4} + \frac{5x}{2} - \frac{\pi^2 x}{2} + \frac{2\pi^2 x^2}{3} \right] , \quad (\text{C.11})
\end{aligned}$$

$$\begin{aligned}
[E, P^{(0)}]_{gq} = & b_0 C^{qq}(x) + C_F n_f \left[(1+x) (\log^2 x + 2 \text{Li}_2(x)) \right. \\
& + \frac{1}{3} \left(20 - \pi^2 - \frac{2}{x} - 2x - \pi^2 x - 16x^2 \right) \\
& + \left(1 + 5x - \frac{4x^2}{3} \right) \log x - \left(1 + \frac{4}{3x} - x - \frac{4x^2}{3} \right) \log(1-x) \left. \right] \\
& + C_F^2 \left[\left(\frac{27}{4} - 4\zeta(3) \right) \delta(1-x) + 3 \left(\frac{\log(1-x)}{1-x} \right)_+ + \frac{3}{2} \log^2 x \right. \\
& - \left. \left(12 - \frac{6}{x} + \frac{5x}{2} \right) \log(1-x) + \left(2 - \frac{2}{x} - x \right) \log^2(1-x) - \frac{9}{2} - \frac{\pi^2}{2} + \frac{3x}{2} \right]
\end{aligned}$$

$$\begin{aligned}
& - 2 \left(2 - \frac{2}{x} - x \right) \log x \log(1-x) - \left(1 - \frac{4}{x} - 2x \right) \text{Li}_2(x) + \left(\frac{7}{2} + 4x \right) \log x \\
& - (1+x^2) \left[3 \left(\frac{\log^2(1-x)}{1-x} \right)_+ + \frac{\log^2 x}{1-x} - 4 \frac{\log x \log(1-x)}{1-x} \right] \\
& - \frac{3}{2} (1-x^2) \frac{\log x}{1-x} + \left(\frac{27}{4} + \frac{2\pi^2}{3} + \frac{9x^2}{2} + \frac{2\pi^2 x^2}{3} \right) \left(\frac{1}{1-x} \right)_+ \\
& + C_A C_F \left[-6 \left(\frac{\log(1-x)}{1-x} \right)_+ + 3 \frac{\log x}{1-x} + \left(\frac{\pi^2}{2} + 4\zeta(3) \right) \delta(1-x) \right. \\
& + 2 \left(1 - \frac{2}{x} - 2x \right) \text{Li}_2(x) - 8x \frac{\log x \log(1-x)}{1-x} + 6x \left(\frac{\log^2(1-x)}{1-x} \right)_+ \\
& + 2x \frac{\log^2 x}{1-x} - \left(9x + \frac{4\pi^2 x}{3} \right) \left(\frac{1}{1-x} \right)_+ - (1+2x^2)(3 \log x + \log^2 x) \\
& + \left(\frac{2}{x} - 2x^2 \right) \log^2(1-x) + \left(2 - \frac{4}{x} - 2x + 4x^2 \right) \log x \log(1-x) \\
& \left. + \left(17 - \frac{6}{x} - 4x + 6x^2 \right) \log(1-x) - 2 - 6x + \frac{\pi^2 x}{3} + 8x^2 + \frac{2\pi^2 x^2}{3} \right]. \quad (\text{C.12})
\end{aligned}$$

Finally

$$[E, P^{(0)}]_{gg} = - [E, P^{(0)}]_{qq} . \quad (\text{C.13})$$

D Truncated moment integrals

The integrals which are needed in order to compute the Mellin moments of the NLO Altarelli-Parisi splitting functions are well known [15]. Here we list all the truncated moment integrals which are necessary in order to determine the evolution kernels $G_n(x)$, eq. (2.5), from the expressions of the splitting functions given in appendix C. The triangular anomalous dimension matrices C_{kl} , eq. (2.12), can be easily determined from these formulas by Taylor expansion.

$$\int_x^1 dz z^{n-1} = \frac{1-x^n}{n} , \quad (\text{D.1})$$

$$\int_x^1 dz z^{n-1} \log z = -\frac{1-x^n(1-n \log x)}{n^2} , \quad (\text{D.2})$$

$$\int_x^1 dz z^{n-1} \log^2 z = \frac{2-x^n(2-2n \log x + n^2 \log^2 x)}{n^3} , \quad (\text{D.3})$$

$$\begin{aligned}
\int_x^1 dz z^{n-1} \log(1-z) &= -\frac{1}{n(n+1)} \left[x^{n+1} {}_2F_1(n+1, 1; n+2; x) \right. \\
&\quad \left. + (n+1) (\gamma_E + x^n \log(1-x) + \psi^{(0)}(n+1)) \right] , \quad (\text{D.4})
\end{aligned}$$

$$\int_x^1 dz z^{n-1} \log z \log(1-z) = -\frac{1}{n^2} \left[-\gamma_E - n x^{n+1} \Phi(x, 2, n+1) - x^n \log(1-x) \right] \quad (\text{D.5})$$

$$\begin{aligned}
& + n x^n \log(1-x) \log x + x^{n+1} \Phi(x, 1, n+1) (n \log x - 1) \\
& + \psi^{(0)}(n) + n [\psi^{(0)}(n)]^2 - n [\psi^{(0)}(n+1)]^2 + n \psi^{(1)}(n+1) \Big] ,
\end{aligned}$$

$$\begin{aligned}
\int_x^1 dz z^{n-1} \frac{\log z}{1-z} &= \frac{x^n}{n^2} + x^{n+1} \Phi(x, 2, n+1) - \frac{x^n}{n} \log x \\
& - x^{n+1} \Phi(x, 1, n+1) \log x - \psi^{(1)}(n) ,
\end{aligned} \tag{D.6}$$

$$\begin{aligned}
\int_x^1 dz z^{n-1} \frac{\log^2 z}{1-z} &= -\frac{2x^n}{n^3} - 2x^{n+1} \Phi(x, 3, n+1) + \frac{2x^n}{n^2} \log x \\
& + 2x^{n+1} \Phi(x, 2, n+1) \log x - \frac{x^n}{n} \log^2 x \\
& - x^{n+1} \Phi(x, 1, n+1) \log^2 x - \psi^{(2)}(n) ,
\end{aligned} \tag{D.7}$$

$$\int_x^1 dz z^{n-1} \left(\frac{1}{1-z} \right)_+ = -\gamma_E - \frac{x^n}{n} {}_2F_1(1, n; n+1; x) - \psi^{(0)}(n) , \tag{D.8}$$

$$\begin{aligned}
\int_x^1 dz z^{n-1} \frac{\log z \log(1-z)}{1-z} &= \text{Li}_3(1-x) - \log(1-x) \text{Li}_2(1-x) \\
& - \sum_{k=1}^{n-1} \int_x^1 dz z^{k-1} \log z \log(1-z) ,
\end{aligned} \tag{D.9}$$

$$\begin{aligned}
\int_x^1 dz z^{n-1} \frac{1}{1+z} &= -\frac{x^n}{n} {}_2F_1(n, 1; n+1; -x) \\
& - \frac{1}{2} \left[\psi^{(0)}\left(\frac{n}{2}\right) - \psi^{(0)}\left(\frac{n+1}{2}\right) \right] ,
\end{aligned} \tag{D.10}$$

$$\begin{aligned}
\int_x^1 dz z^{n-1} \frac{\log z \log(1+z)}{1+z} &= (-1)^{n-1} \left[-\frac{\zeta(3)}{8} - \frac{\log x \log^2(1+x)}{2} + \frac{\log^3(1+x)}{3} \right. \\
& + \log(1+x) \text{Li}_2\left(\frac{x}{1+x}\right) + \text{Li}_3(-x) + \text{Li}_3\left(\frac{x}{1+x}\right) \\
& \left. - \sum_{k=1}^{n-1} (-1)^{k-1} \int_x^1 dz z^{k-1} \log z \log(1+z) \right] ,
\end{aligned} \tag{D.11}$$

$$\begin{aligned}
\int_x^1 dz z^{n-1} \frac{\log^2 z}{1+z} &= -\frac{2x^n}{n^3} + 2x^{n+1} \Phi(-x, 3, n+1) \\
& + \frac{2}{n^2} x^n \log x - 2x^{n+1} \Phi(-x, 2, n+1) \log x \\
& - \frac{x^n}{n} \log^2 x + x^{n+1} \Phi(-x, 1, n+1) \log^2 x \\
& - \frac{1}{8} \left[\psi^{(2)}\left(\frac{n}{2}\right) - \psi^{(2)}\left(\frac{n+1}{2}\right) \right] ,
\end{aligned} \tag{D.12}$$

$$\begin{aligned}
\int_x^1 dz z^{n-1} \frac{\text{Li}_2(-z)}{1+z} &= (-1)^{n-1} \left[-\frac{7\zeta(3)}{4} - \frac{\pi^2}{12} \log 2 + \log(1+x) \text{Li}_2(-x) \right. \\
& + \log x \log^2(1+x) + \frac{\pi^2}{3} \log(1+x) + 2\text{Li}_3\left(\frac{1}{1+x}\right) \\
& \left. - \sum_{k=1}^{n-1} (-1)^{k-1} \int_x^1 dz z^{k-1} \text{Li}_2(-z) \right] ,
\end{aligned}$$

$$-\frac{\log^3(1+x)}{3} - \sum_{k=1}^{n-1} (-1)^{k-1} \int_x^1 dz z^{k-1} \text{Li}_2(-z) \Big] , \quad (\text{D.13})$$

$$\begin{aligned} \int_x^1 dz z^{n-1} \log z \log(1+z) &= \frac{1}{4n^2} \left[-4n x^{n+1} \Phi(-x, 2, n+1) - 4 \log 2 \right. \\ &\quad + 4x^{n+1} \Phi(-x, 1, n+1) (-1 + n \log x) + 4x^n \log(1+x) \\ &\quad - 4n x^n \log x \log(1+x) + 2\psi^{(0)}\left(1 + \frac{n}{2}\right) - 2\psi^{(0)}\left(\frac{n+1}{2}\right) \\ &\quad \left. - n\psi^{(1)}\left(1 + \frac{n}{2}\right) + n\psi^{(1)}\left(\frac{n+1}{2}\right) \right] , \end{aligned} \quad (\text{D.14})$$

$$\begin{aligned} \int_x^1 dz z^{n-1} \left(\frac{\log(1-z)}{1-z} \right)_+ &= (n-1)(1-x) \left[{}_4F_3(1, 1, 1, 2-n; 2, 2, 2; 1-x) \right. \\ &\quad \left. - {}_3F_2(1, 1, 2-n; 2, 2; 1-x) \log(1-x) \right] + \frac{\log(1-x)^2}{2} , \end{aligned} \quad (\text{D.15})$$

$$\begin{aligned} \int_x^1 dz z^{n-1} \text{Li}_2(-z) &= \frac{1}{n^2(n+1)} \left[x^{n+1} {}_2F_1(n+1, 1; n+2; -x) \right. \\ &\quad - (n+1) \left(\frac{n\pi^2}{12} - \log 2 + x^n \log(1+x) \right. \\ &\quad \left. \left. + \frac{1}{2} \left[\psi^{(0)}\left(1 + \frac{n}{2}\right) - \psi^{(0)}\left(\frac{n+1}{2}\right) \right] + n x^n \text{Li}_2(-x) \right) \right] , \end{aligned} \quad (\text{D.16})$$

$$\begin{aligned} \int_x^1 dz z^{n-1} \log^2(1-z) &= 2(1-x) \left[{}_4F_3(1, 1, 1, 1-n; 2, 2, 2; 1-x) \right. \\ &\quad - {}_3F_2(1, 1, 1-n; 2, 2; 1-x) \log(1-x) \Big] \\ &\quad + \frac{1-x^n}{n} \log^2(1-x) , \end{aligned} \quad (\text{D.17})$$

$$\begin{aligned} \int_x^1 dz z^{n-1} \text{Li}_2(z) &= \frac{1}{n^2 \Gamma(n+2)} \left[-\Gamma(2+n) (\gamma_E + \psi^{(0)}(n+1)) \right. \\ &\quad + \Gamma(n+1) \left(-x^{n+1} {}_2F_1(n+1, 1; n+2; x) \right. \\ &\quad \left. \left. + (n+1) \left(n \frac{\pi^2}{6} - x^n \log(1-x) - n x^n \text{Li}_2(x) \right) \right) \right] , \end{aligned} \quad (\text{D.18})$$

$$\begin{aligned} \int_x^1 dz z^{n-1} \left(\frac{\log^2(1-z)}{1-z} \right)_+ &= \frac{\log(1-x)^3}{3} - (1-x) \sum_{j=0}^{n-2} \left[2 {}_4F_3(1, 1, 1, -j; 2, 2, 2; 1-x) \right. \\ &\quad - 2 {}_3F_2(1, 1, -j; 2, 2; 1-x) \log(1-x) \\ &\quad \left. + \frac{1-x^{j+1}}{(j+1)(1-x)} \log^2(1-x) \right] , \end{aligned} \quad (\text{D.19})$$

where

$$\text{Li}_m(z) = \sum_{k=1}^{\infty} \frac{z^k}{k^m} ; \quad \text{Li}_2(z) = \int_z^0 dt \frac{\log(1-t)}{t} ; \quad (\text{D.20})$$

$$\psi^{(k)}(n) = \frac{d^{k+1} \log \Gamma(n)}{dn^{k+1}} ; \quad \gamma_E = -\psi^{(0)}(1) \approx 0.577216 ; \quad (D.21)$$

$$\Phi(z, s, a) = \sum_{k=0}^{\infty} \frac{z^k}{(a+k)^s} ; \quad (D.22)$$

$${}_pF_q(a_1, \dots, a_p; b_1, \dots, b_q; z) = \sum_{k=0}^{\infty} \frac{(k+a_1) \dots (k+a_p)}{(k+b_1) \dots (k+b_q)} \frac{z^k}{k!} . \quad (D.23)$$

Note that the integrals in eqs. (D.9), (D.11), (D.13) and (D.19) are valid only when n is a positive integer, which is what is usually needed. If an expression for real or complex n is necessary, one should compute these integrals numerically. All other integrals are given in a form that immediately generalizes to complex n . The special functions in eqs. (D.20-D.23) are available in algebraic manipulation programs of common use.

References

- [1] See *e.g.* S. Catani *et al.*, [hep-ph/0005025](#), to be published in the proceedings of the workshop “Standard Model Physics (and more) at the LHC” (CERN, 1999).
- [2] See *e.g.* S. Forte, *Nucl. Phys.* **A666** (2000) 113.
- [3] See *e.g.* R.K. Ellis, W.J. Stirling and B.R. Webber, “QCD and Collider Physics” (C.U.P., Cambridge, 1996).
- [4] S. A. Larin *et al.*, *Nucl. Phys.* **B492** (1997) 338, [hep-ph/9605317](#).
- [5] E. B. Zijlstra and W. L. van Neerven, *Nucl. Phys.* **B383** (1992) 525.
- [6] G. Altarelli and G. Parisi, *Nucl. Phys.* **B126** (1977) 298.
- [7] G. Altarelli, R. K. Ellis and G. Martinelli, *Nucl. Phys.* **B143** (1978) 521; **B157** (1979) 461.
- [8] S. Catani, *Z. Phys.* **C75** (1997) 665, [hep-ph/9609263](#).
- [9] W. T. Giele and S. Keller, *Phys. Rev.* **D58** (1998) 094023, [hep-ph/9803393](#); D. Kosower, W. T. Giele and S. Keller, Proc. of the 1999 “Rencontres de Physique de la Vallée d’Aoste”, pag. 255 (INFN, Frascati, 1999); R. D. Ball and J. Huston, in S. Catani *et al.*, [hep-ph/0005114](#).
- [10] G. Altarelli *et al.*, *Nucl. Phys.* **B496**, 337 (1997), [hep-ph/9701289](#); *Acta Phys. Pol.* **B29** (1998) 1145, [hep-ph/9803237](#).
- [11] F.J. Yndurain, *Phys. Lett.* **B74** (1978) 68; G. Parisi, N. Sourlas, *Nucl. Phys.* **B151** (1979) 421; W. Furmanski, R. Petronzio, *Nucl. Phys.* **B195** (1982) 237.
- [12] S. Forte and L. Magnea, *Phys. Lett.* **B448** (1999) 295, [hep-ph/9812479](#); in Proceedings of the International Europhysics Conference on High-Energy Physics (EPS-HEP 99), Tampere 1999, [hep-ph/9910421](#).
- [13] See *e.g.* Encyclopedic Dictionary of Mathematics, ed. by S. Iyanaga and Y. Kawada, M.I.T. Press (Cambridge, Mass., 1980).
- [14] M. Diemoz, S. Ferroni, M. Longo and G. Martinelli, *Z. Phys.* **C39** (1988) 20.
- [15] For comprehensive tables see *e.g.* A. Devoto and D. W. Duke, *Riv. Nuovo Cim.* **7** (1984) 1; J. Blümlein and S. Kurth, *Phys. Rev.* **D60** (1999) 014018, [hep-ph/9810241](#).